The Astrophysical Journal, 871:119 (4pp), 2019 January 20 https://doi.org/10.3847/1538-4357/aaf6aa


# Measuring the Absolute Total Intrinsic Redshifts (Surface Gravity Plus the Convective Blueshift) of the Main-sequence Stars and Red Giants using *Gaia* Data

De-Chang Dai[1,3], ZhiGang Li[2,4], and Dejan Stojkovic[5]
[1] Center for Gravity and Cosmology, School of Physics Science and Technology, Yangzhou University, 180 Siwangting Road, Yangzhou City, Jiangsu Province, 225002, People's Republic of China; diedachung@gmail.com
[2] College of Physics and Electronic Engineering, Nanyang Normal University, Nanyang, Henan, 473061, People's Republic of China; zhigli@sjtu.edu.cn
[3] CERCA/Department of Physics/*ISO*, Case Western Reserve University, Cleveland, OH 44106-7079, USA
[4] Department of astronomy, Shanghai Jiao Tong University, Shanghai 200240, People's Republic of China
[5] HEPCOS, Department of Physics, SUNY at Buffalo, Buffalo, NY 14260-1500, USA
*Received 2018 October 21; revised 2018 December 1; accepted 2018 December 4; published 2019 January 25*

## Abstract

We analyze the *GAIA* release II data to demonstrate how one can measure the absolute total intrinsic redshifts of the main-sequence stars and red giants. We remove the relative velocity components of the stars' motion with respect to the Sun by doing the analysis in the local standard of the rest frame defined by the average stars' motion. We provide results for four different types of stars. F-, G-, and K-type stars have about the same value of intrinsic redshift, which is, however, much smaller than the expected gravitational redshift. This indicates that *GAIA*'s data includes a convective blueshift effect of a several hundred m $s^{-1}$ magnitude. The red giants' intrinsic redshifts are negative, which implies that their convective blueshift is stronger than the gravitational redshift. This is expected since red giants are far less compact than other types.

*Key words:* gravitation

## 1. Introduction

Various techniques utilized in observational astrophysics enabled us to measure general relativistic effects such as the gravitational redshift of distant stars. The first confirmed measurement of the gravitational redshift of a distant star comes from the measurement of the apparent radial velocity of a while dwarf, Sirius B (Adams 1925). The Sun's gravitational redshift has also been measured (see a review in Takeda & Ueno 2012). Recently the gravitational redshift was observed from the star S2 orbiting around the massive black hole candidate SgrA$^*$ (Gravity Collaboration et al. 2018). Apart from the Sun, which is the closest, and white dwarfs that have very strong gravitational redshift, it is possible to measure gravitational redshift in a group of comoving stars by comparing the average redshifts of different types of stars and removing the (Doppler) velocity redshift. A shortcoming of this method is that it provides only a relative gravitational redshift rather than an absolute. In addition, it was found in Pasquini et al. (2011) that the M67 open cluster does not produce an expected signal. The discrepancy can be caused by the convective blueshift, which is wavelength dependent (Meunier et al. 2017a, 2017b). It is also possible to measure radial velocities using astrometric methods without involving spectroscopic data (Dravins et al. 1999). The intrinsic redshift can be extracted by comparing astrometric and spectroscopic radial velocities. Based on this method, Leão et al. studied the Hyades open cluster and found that red giants have more blueshifted spectra than the dwarfs (Leão et al. 2018). However, there are very few data sets that include both spectroscopic and astrometric radial velocities, so methods based on analyzing only spectroscopic radial velocities data are still very useful.

In this paper we demonstrate how one can extract absolute total intrinsic redshifts of the main-sequence stars and red giants. This intrinsic redshift is usually dominated by the surface gravity of the star (which is purely a general relativistic effect), however it also includes the convective blueshift, which cannot be easily removed without additional information. A straightforward way to measure the total redshift effect is to observe a star at rest with respect to us. This is practically impossible due to the stars relative motion with respect to the Sun. However, we can circumvent the problem using a local standard of rest (LSR) frame as the coordinate system of the average stars' motion (Schönrich et al. 2010; Coşkunoğlu et al. 2011; Huang et al. 2015). Then, we can use these coordinates to study the gravitational redshift. Such a procedure was previously utilized in Falcon et al. (2010) to analyze the gravitational redshift of 449 non-binary white dwarfs. Since the gravitational redshift of white dwarfs is 2–3 orders of magnitude stronger than that of the main-sequence stars, several hundred stars are enough for the procedure to work. For the same method to be useful for the main-sequence stars, this number must be much higher.

## 2. Data and Method

In this work we use the *GAIA* data release II. The *GAIA* sky survey charts a three-dimensional map of our Galaxy, the Milky Way, revealing the composition, formation, and evolution of the Galaxy (Gaia Collaboration et al. 2016, 2018a). The star morphology can be obtained from the Hertzsprung-Russell (HR)-diagrams in Gaia Collaboration et al. (2018b) and Gaia Collaboration et al. (2018). In our study, we concentrate on the kinematics information of the nearby stars. The HR-diagram for stars within 1 kpc from the Sun is shown in Figure 1. Most of the stars' surface temperatures range are from 3500k to 8000k. This covers the F-, G-, K-, and red giant types, and therefore we will mainly focus on these four groups.

The *GAIA* data provides the total redshift of the stars. This means that both the gravitational and Doppler redshift effects are included. To distinguish between these two effects, the redshift velocity, $V_r$ (Cropper et al. 2018; Katz et al. 2018; Soubiran et al. 2018), and the transverse velocity, $V_{\mathrm{R.A.}}$ and

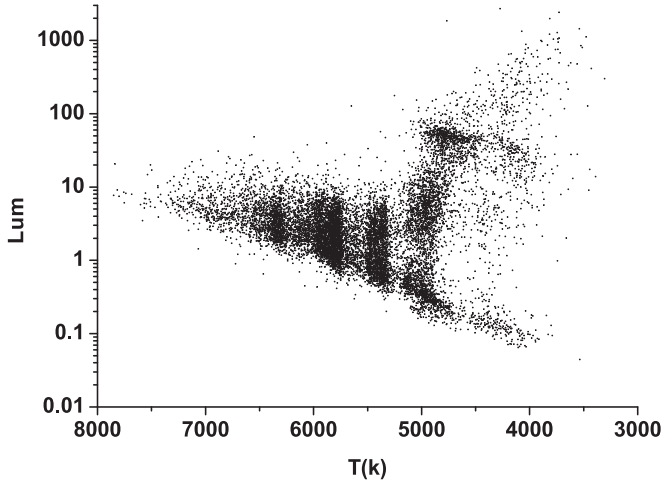


**Figure 1.** This HR-diagram includes stars whose distance to the Sun is from 0.05 to 1 kpc. Only a small fraction (1/200) of stars we use are drawn in this diagram.

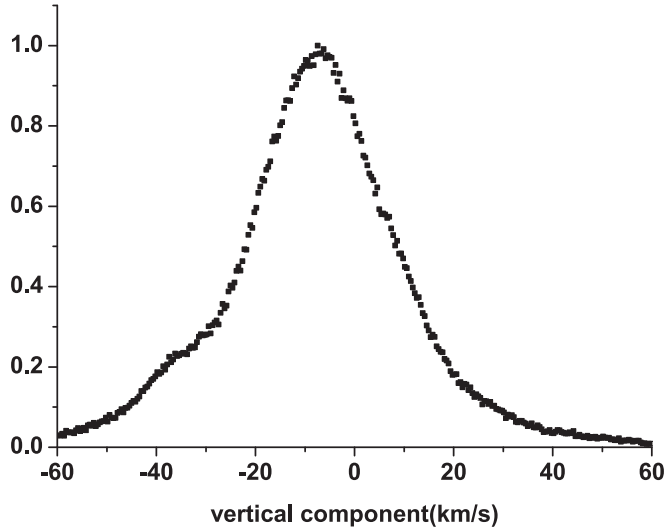


**Figure 2.** Distribution of the vertical velocity components of the stars (Equation (2)). The distances between the stars and the Sun range from 0.05 kpc to 0.5 kpc. Only stars with temperatures between 5200 and 6000 K (G-type stars) and a radius between 0.8 and 1.2 are included. The distribution is normalized to a maximum magnitude of one.

$V_{\rm Decl.}$ (in the R.A. and decl. direction), must be considered simultaneously. $V_{\rm R.A.}$ and $V_{\rm Decl.}$ are measured relative to the Sun and $V_r$ is measured from the star's spectral redshift, which does not directly represent the relative velocity to the Sun along the line-of-sight direction. $V_r$ includes the Doppler redshift due to the star's motion, gravitational redshift, and convective blueshift due to the motion of the material close to the star's surface. We can separate $V_r$ in two components as

$$V_r = v_r + v_s. \tag{1}$$

Here, $v_r$ is the star's relative velocity with respect to the Sun along the line-of-sight direction, while $v_s$ is the combination of the star's gravitational redshift, $v_g$, and convective blueshift, $v_c$. The $v_g$ component is about the same for the same type of stars, since the star's mass and radius do not change much within the class. However, $v_c$ can be strongly dependent on the observation wavelength (Meunier et al. 2017a, 2017b). It was found in Meunier et al. (2017a, 2017b) that the convective blueshift can be several hundreds of $\mathrm{m\,s^{-1}}$ in *GAIA*'s wavelength region. In principle, many additional effects can affect the results. For example, the gravitational potential of the galaxy can affect the radial velocity measurements (Lindegren & Dravins 2003). However, since our stars are within 1 kpc, the redshift from the gravitational potential of the Milky Way is only several tens of $\mathrm{m\,s^{-1}}$. This is one order of magnitude smaller than $v_r$, so we neglect it in the study. Relativistic effects due to the difference between the proper and coordinate time (as defined by an adopted metric) can also affect the radial velocity measurement. However, this effect is about several $\mathrm{m\,s^{-1}}$ and can be safely neglected in our study (Lindegren & Dravins 2003; Leão et al. 2018). Stellar rotation and activity can also affect the spectral radial velocity measurement. The magnitude of the stellar rotation effect is expected to be about several $10\,\mathrm{m\,s^{-1}}$ in Leão et al. (2018), though Lindegren & Dravins expect a value of several $100\,\mathrm{m\,s^{-1}}$ (Lindegren & Dravins 2003). Since it is very difficult to have such detailed information about every single star, we just assume that these effects are randomly distributed and therefore are statistically canceled out. Finally, the effect of stellar activity is expected to be several $10\,\mathrm{m\,s^{-1}}$ (Lindegren & Dravins 2003; Leão et al. 2018). It appears that the surface gravitational redshift and convection blueshift are the dominant effects, while the other effects are smaller than our precision, so we primarily focus on them.

Our main goal is to extract $v_s$ from $V_r$, $V_{\rm R.A.}$, and $V_{\rm Decl.}$. It is possible to remove the relative velocity components by doing the analysis in the LSR frame. The velocity of a star in this frame can be labeled as ($U$, $V$, $W$), where $U$, $V$, and $W$ are velocities in the galactic radial, rotational, and vertical direction, respectively. Accordingly, the velocity of the Sun in the same frame is ($U_\odot$, $V_\odot$, $W_\odot$). In the LSR frame, all of the stars are moving in a group, and the average values of all three components, $\bar{U}$, $\bar{V}$, and $\bar{W}$, should not be far from 0. Unfortunately, this is not completely correct. The $U$ and $V$ components are more complicated (Schönrich et al. 2010; Francis & Anderson 2014), since $U$ is not completely symmetric (Schönrich et al. 2010), and the galaxy is expanding in radial direction (Siebert et al. 2011). Thus, the contribution of $U$ and $V$ on measuring $v_s$ is not easily estimated. $W$ on the other hand is expected to be symmetric, since the Milky Way is basically cylindrically symmetric. We therefore analyze the stars velocities in the vertical direction. The vertical component is then

$$(V_r\hat{r} + V_{\rm Decl.}\hat{\delta} + V_{\rm R.A.}\hat{\alpha}) \cdot \hat{z} = W - W_\odot + v_s\cos(b). \tag{2}$$

Here, $\delta$ and $\alpha$ are the decl. and R.A. in the equatorial coordinate system, respectively. $\hat{r}$, $\hat{\delta}$, and $\hat{\alpha}$ are the unit vectors in three relevant directions. $\hat{z}$ is the galactic north pole direction. The decl. and R.A. of the galactic north pole's direction are $\alpha_g = 192.^\circ85948$ and $\delta_g = 27.^\circ12825$. $b$ is the galactic latitude. The right-hand side of Equation (2) is the theoretical expectation, while the left-hand side is what we fit. Since the values of $W$ are randomly distributed, they can be treated as noise, while the relevant information to be extracted is in quantities of $v_s$ and $W_\odot$. Figure 2 shows the left-hand side

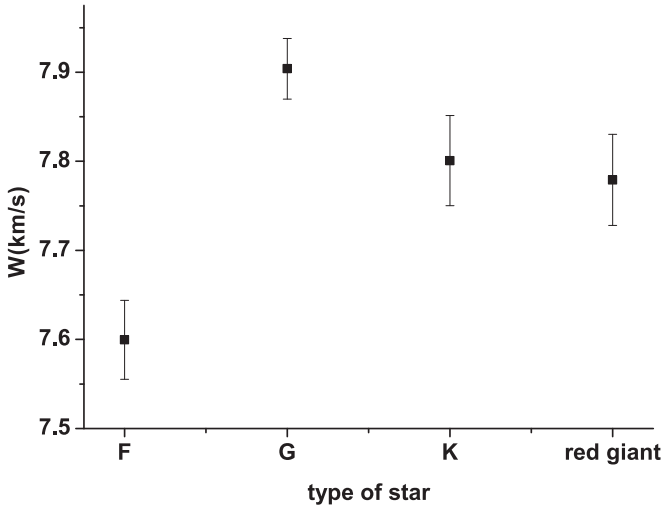


**Figure 3.** Vertical velocity of the Sun, $W_\odot$, with respect to the LSR. The error bars are $1\sigma$. The values for $W_\odot$ are quite consistent for the four different types of stars (F, G, K, and red giants).

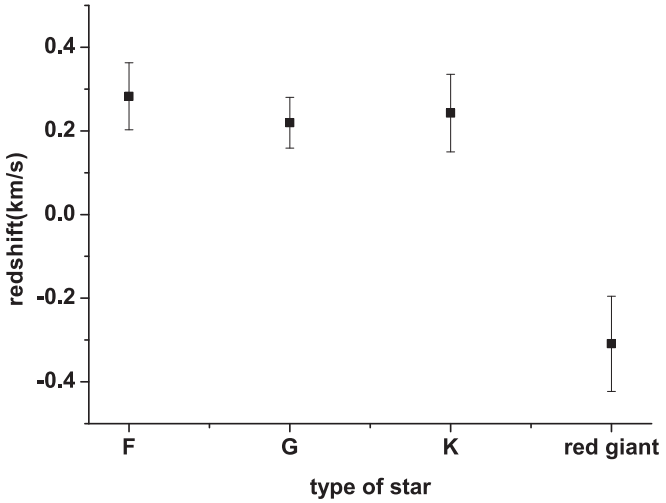


**Figure 4.** We plot here the total intrinsic redshift (gravitational plus convective blueshift) represented by the velocity $v_s$ for the different types of stars. The error bars are $1\sigma$. The redshift values for the red giants are negative, which implies that their convective blueshift is stronger than the gravitational redshift. F, G, and K types have about the same value of $v_s$, which is larger than that for the red giants value. The gravitational redshift difference between the Sun and a 10 solar radii giant is about 570 m s$^{-1}$. The difference can be larger for an even larger red giant. The difference in $v_s$ values between G-type stars and red giants is $\Delta v_s = 0.53 \pm 0.13$ km s$^{-1}$, which is consistent with the expected difference coming from the gravitational redshift ($\approx$600 m s$^{-1}$), though the exact convection blueshift contribution is not known here.

of Equation (2). The distribution is practically spherically symmetric, except some small bumps.

The data are separated into four different groups corresponding to different types of stars: F, G, K, and red giants. F-type stars include star surface temperatures from 6000 K to 7500k, and star radii from 1.15 $R_\odot$ to 1.4 $R_\odot$. We use a total of 134,697 F-type stars in our analysis. G-type stars include star surface temperatures from 5200 K to 6000k, and star radii from 0.8 $R_\odot$ to 1.2 $R_\odot$. We use a total of 361,157 G-type stars in our analysis. K-type stars include stars surface temperatures from 3700 K to 5200k, and star radii from 0.7 $R_\odot$ to 1 $R_\odot$. We use a total of 137,456 K-type stars in our analysis. Red giant type stars include stars surface temperatures from 3700 K to 5200 k, and star radii larger than 10 $R_\odot$. We use a total of 155,721 red giants in our analysis. All of the stars are between 0.05 pc to 1 kpc away from the Sun. Since the surface gravitational redshift of a main-sequence star is around several hundreds of m s$^{-1}$, and the vertical velocity component is about several tens of km s$^{-1}$, we need tens of thousands of stars to achieve the signal-to-noise ratio around one. We therefore include several hundred thousands of stars of each type in our analysis, which should be enough to study the star's intrinsic redshift effect.

We did not include all of the stars within 1 kpc from the Sun, because the stars' radii are not always given very precisely. Fortunately, the catalog gives the stars' radii for the main-sequence stars and red giants, which is sufficient for the main aim of our study. We choose only stars with radii larger than 10 $R_\odot$ as red giants, in order to avoid overlap with other large stars. We discard all of the other stars. The number of stars we included within these four types is quite sufficient to distinguish the signal from the noise.

## 3. Result

We fit the vertical data with Equation (2) using the standard minimal $\chi^2$ analysis. Both $W_\odot$ and the redshift of a star can be obtained at the same time. The error for each data point is assumed to be the same, and can be estimated from the standard deviation of a vertical component, which is about several tens of km s$^{-1}$. Figure 3 shows $W_\odot$ from the different types of stars. The values for $W_\odot$ for F-type stars are a bit lower than the values for the other types. The apparent difference might come from systematic errors, or from the stars' spatial distribution (Schönrich et al. 2010; Coşkunoğlu et al. 2011; Huang et al. 2015). However, this is still within $3\sigma$, so it should not matter much. In the literature, the measured values for $W_\odot$ range from 3.6 to 10 km s$^{-1}$ (Huang et al. 2015). The result depends on the samples and models used in the analysis. With our fitting strategy, the velocity of the LSR should be close to the average value of stars' vertical motion. Since different types of stars cover different regions of space, this may cause the above mentioned discrepancy.

Figure 4 shows $v_s$ (the total gravitational and convective blueshift) from different types of stars. F, G, and K have about the same $v_s$. This value, however, is much smaller than the expected gravitational redshift, which is about 600 m s$^{-1}$. This may confirm that *GAIA*'s data does indeed include the convective blueshift effect of a several hundreds m s$^{-1}$ magnitude (Meunier et al. 2017a, 2017b). The red giants $v_s$ are much smaller than those of the main-sequence stars. This is consistent with the theoretical prediction. Since red giants $v_s$ are negative, their convective blueshift, $v_c$, must be stronger than its gravitational redshift, $v_g$. This is also expected since red giants radii are much larger, and therefore $v_g$ is expected to be smaller. The difference in $v_s$ values between G-type stars and red giants is $\Delta v_s = 0.53 \pm 0.13$ km s$^{-1}$, which is consistent with the expected difference coming from gravitational redshift ($\approx$600 m s$^{-1}$). We note, however, that in this study we do not know the exact convection blueshift contribution for the different types of stars.

## 4. Conclusion

In conclusion, we presented here the first measurement of the absolute total intrinsic redshifts (which include surface gravity plus the convective blueshift) of main-sequence stars and red giants using *GAIA* data. The obtained values are consistent with

the theoretical expectations. As a next step, it would be very important to separate the surface gravity from the convective blueshift effect. If the mass and radius of a star are known, then one can calculate the gravitational potential and extract the net convective blueshift effect. This can perhaps be done in binary systems.

D.C.D. was supported by the National Science Foundation of China (grant No. 11433001 and 11775140), the National Basic Research Program of China (973 Program 2015CB857001), and the Program of Shanghai Academic/Technology Research Leader under grant No. 16XD1401600. Z.L. was supported by the Project for New faculty of Shanghai Jiao Tong University (AF0720053), the National Science Foundation of China (No. 11533006, 11433001), and the National Basic Research Program of China (973 Program 2015CB857000). D.S. was partially supported by the NSF grant PHY 1820738.

This work has made use of data from the European Space Agency (ESA) mission *Gaia* (https://www.cosmos.esa.int/gaia), processed by the *Gaia* Data Processing and Analysis Consortium (DPAC; https://www.cosmos.esa.int/web/gaia/dpac/consortium). Funding for DPAC has been provided by national institutions, in particular the institutions participating in the *Gaia* Multilateral Agreement.

## References

Adams, W. S. 1925, Obs, 48, 337
Coşkunoğlu, B., Ak, S., Bilir, S., et al. 2011, MNRAS, 412, 1237
Cropper, M., Katz, D., Sartoretti, P., et al. 2018, arXiv:1804.09369
Dravins, D., Lindegren, L., & Madsen, S. 1999, A&A, 348, 1040
Falcon, R. E., Winget, D. E., Montgomery, M. H., & Williams, K. A. 2010, ApJ, 712, 585
Francis, C., & Anderson, E. 2014, CeMDA, 118, 399
Gaia Collaboration, Babusiaux, C., van Leeuwen, F., et al. 2018b, A&A, 616, A10
Gaia Collaboration, Brown, A. G. A., Vallenari, A., et al. 2018a, A&A, 616, A1
Gaia Collaboration, Katz, D., Antoja, T., et al. 2018, A&A, 616, A11
Gaia Collaboration, Prusti, T., de Bruijne, J. H. J., et al. 2016, A&A, 595, A1
Gravity Collaboration, Abuter, R., Amorim, A., et al. 2018, A&A, 615, L15
Huang, Y., Liu, X.-W., Yuan, H.-B., et al. 2015, MNRAS, 449, 162
Katz, D., Sartoretti, P., Cropper, M., et al. 2018, arXiv:1804.09372
Leão, I. C., Pasquini, L., Ludwig, H.-G., & de Medeiros, J. R. 2018, arXiv:1811.08771
Lindegren, L., & Dravins, D. 2003, A&A, 401, 1185
Meunier, N., Lagrange, A.-M., Mbemba Kabuiku, L., et al. 2017a, A&A, 597, A52
Meunier, N., Mignon, L., & Lagrange, A.-M. 2017b, A&A, 607, A124
Pasquini, L., Melo, C., Chavero, C., et al. 2011, A&A, 526, A127
Schönrich, R., Binney, J., & Dehnen, W. 2010, MNRAS, 403, 1829
Siebert, A., Famaey, B., Minchev, I., et al. 2011, MNRAS, 412, 2026
Soubiran, C., Jasniewicz, G., Chemin, L., et al. 2018, A&A, 616, A7
Takeda, Y., & Ueno, S. 2012, SoPh, 281, 551